

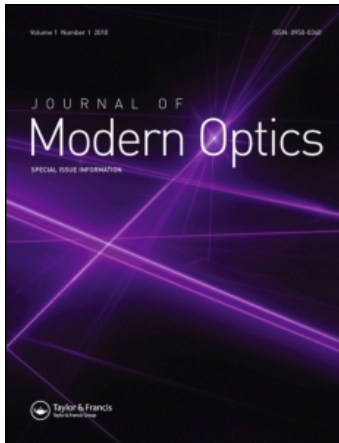
This article was downloaded by: [Centro Ciencias Aplicadas Y Des]

On: 22 February 2011

Access details: Access Details: [subscription number 918400151]

Publisher Taylor & Francis

Informa Ltd Registered in England and Wales Registered Number: 1072954 Registered office: Mortimer House, 37-41 Mortimer Street, London W1T 3JH, UK



Journal of Modern Optics

Publication details, including instructions for authors and subscription information:

<http://www.informaworld.com/smpp/title~content=t713191304>

Nonlinear optical performance of poled liquid crystalline azo-dyes confined in SiO₂ sonogel films

V. Torres-Zúñiga^a; O. G. Morales-Saavedra^a; E. Rivera^b; J. O. Flores-Flores^a; J. G. Bañuelos^a; R. Ortega-Martínez^b

^a Centro de Ciencias Aplicadas y Desarrollo Tecnológico, Universidad Nacional Autónoma de México, D.F. México ^b Instituto de Investigaciones en Materiales, Universidad Nacional Autónoma de México, D.F. México

Online publication date: 03 February 2010

To cite this Article Torres-Zúñiga, V. , Morales-Saavedra, O. G. , Rivera, E. , Flores-Flores, J. O. , Bañuelos, J. G. and Ortega-Martínez, R.(2010) 'Nonlinear optical performance of poled liquid crystalline azo-dyes confined in SiO₂ sonogel films', Journal of Modern Optics, 57: 1, 65 — 73

To link to this Article: DOI: 10.1080/09500340903521843

URL: <http://dx.doi.org/10.1080/09500340903521843>

PLEASE SCROLL DOWN FOR ARTICLE

Full terms and conditions of use: <http://www.informaworld.com/terms-and-conditions-of-access.pdf>

This article may be used for research, teaching and private study purposes. Any substantial or systematic reproduction, re-distribution, re-selling, loan or sub-licensing, systematic supply or distribution in any form to anyone is expressly forbidden.

The publisher does not give any warranty express or implied or make any representation that the contents will be complete or accurate or up to date. The accuracy of any instructions, formulae and drug doses should be independently verified with primary sources. The publisher shall not be liable for any loss, actions, claims, proceedings, demand or costs or damages whatsoever or howsoever caused arising directly or indirectly in connection with or arising out of the use of this material.

Nonlinear optical performance of poled liquid crystalline azo-dyes confined in SiO₂ sonogel films

V. Torres-Zúñiga^{a*}, O.G. Morales-Saavedra^a, E. Rivera^b, J.O. Flores-Flores^a, J.G. Bañuelos^a and R. Ortega-Martínez^b

^aCentro de Ciencias Aplicadas y Desarrollo Tecnológico, Universidad Nacional Autónoma de México, CCADET-UNAM, A.P. 70-186, Coyoacán 04510, Mexico, D.F. México; ^bInstituto de Investigaciones en Materiales, Universidad Nacional Autónoma de México, IIM-UNAM, A.P. 70-360, Coyoacán 04510, Mexico, D.F. México

(Received 19 August 2009; final version received 27 November 2009)

The catalyst-free sonogel route was implemented to fabricate highly pure, optically active, hybrid azo-dye/SiO₂-based spin-coated thin films deposited onto ITO-covered glass substrates. The implemented azo-dyes exhibit a push-pull structure; thus chromophore electrical poling was performed in order to explore their quadratic nonlinear optical (NLO) performance and the role of the SiO₂ matrix for allowing molecular alignment within the sonogel host network. Morphological and optical characterizations were performed to the film samples according to atomic force microscopy (AFM), ultraviolet-visible (UV-Vis) spectroscopy and the Maker-fringe technique. Regardless of absence of a high glass transition temperature (T_g) in the studied monomeric liquid crystalline azo-dyes, some hybrid films displayed stable NLO activity such as second harmonic generation (SHG). Results show that the chromophores were homogeneously embedded within the SiO₂ sonogel network, where the guest-host molecular and mechanical interactions permitted a stable monomeric electrical alignment in this kind of environment.

Keywords: hybrid materials; thin films; azobenzene; sol-gel; sonogel; nonlinear optics

1. Introduction

Nonlinear optics is projected to play a central role in the technological fields of electro-optic modulation, optical switching, and optical information processing, among other areas [1–3]. These applications can be performed, based on, for example, second-order nonlinear optical phenomena such as the electro-optical effect and optical SHG [4,5].

Second-order nonlinear optical materials ($\chi^{(2)}$ -NLO) include both inorganic and organic crystals, polymers, and recently artificial hybrid organic-inorganic composites. In particular, azo-dye and azopolymer materials have attracted considerable attention from many research groups in recent years because they represent a promising alternative for NLO applications compared to the pure inorganic crystalline structures. In fact, these organic materials can exhibit enhanced susceptibilities, fast response times, lower dielectric constants, and more versatile processability characteristics [4,6–8]. According to Rau, azobenzenes bearing both electron-donor and electron-acceptor groups belong to the ‘pseudostilbenes’ category, where the π - π^* and n - π^* bands are practically superimposed, both are actually inverted on the energy scale with respect to the non-substituted azobenzenes

bands [9]. Donor-acceptor substituted azobenzenes alone or incorporated into polymer systems provide very versatile materials from an application perspective. It is well documented that highly polar azobenzenes exhibit strong $\chi^{(2)}$ -NLO properties such as SHG [10,11]. The innovation in the design and obtention of more polar azobenzenes constitute a fertile and growing field of research.

On the other hand, it is well known that organic second-order NLO materials must contain optical chromophores, which have to be arranged macroscopically in a non-centrosymmetric manner. Such highly ordered arrangements can be achieved by self-assembly techniques [12,13], electrical poling by high voltage DC fields [14,15], or by building Langmuir-Blodgett films in the case of amphiphilic molecules [16,17].

However, aligned NLO chromophores in polymeric materials are susceptible to thermal relaxation, which tends to annihilate the $\chi^{(2)}$ -NLO response of the materials. Many efforts, including the cross-linking method and the use of high glass transition polymers have been made to prevent the relaxation of NLO molecules in the polymeric matrix, for the purpose of fabricating thermally stable NLO polymeric materials [18,19]. So far, there is no dominating method to

*Corresponding author. Email: vicentz@gmail.com

stabilize permanently a specific kind of NLO chromophores, only a group of proposals for each active molecule.

A route to improve the thermal and mechanical molecular stability is the use of sol-gel matrices to protect the active chromophores for example from environmental degradation. In the last decades, hybrid organic-inorganic materials through several sol-gel processes have been highlighted [20], particularly the inherent properties of silica based sol-gel matrices have lead to some important improvements in the measurements of second-order susceptibilities which are comparable to those of inorganic crystals [21–23]. A novel course in the synthesis of sol-gel glasses is the catalyst-free sonogel route, which consists in the exclusive use of ultrasonic irradiation (UI) in the interface of two reactants: distilled water and TEOS ($\text{H}_2\text{O}/\text{tetraethoxysilane}$) [24]. Due to the absence of basic or acidic catalysts, the UI produces acoustical cavitation and induces sonochemical reactions which lead to the production of a highly pure sol-gel product. The obtained sonochemical product is a colloidal sol-phase which provides, at room temperature, an optimal environment for the inclusion of different optically active organic dopant species [25]. After a slow drying process condensation occurs, thus rigid hybrid structures can be obtained in both thin film samples and monolithic bulk materials containing the dopant molecules of interest. Hence, sonogel technology provides an attractive route to prepare NLO chromophore-containing molecular networks, indeed the use of an inorganic and transparent sol-gel material provides an inert host matrix suitable for optical applications and sample manipulation. Here, the thermal decomposition for the organic chromophores may be prevented [26].

In the present work, we provide detailed experimental evidence concerning the possibility to fabricate stable organic-inorganic NLO active hybrid thin films implementing a SiO_2 based sonogel network and three functionalized rod-like and optically active liquid crystalline (LC) azobenzene molecular systems (azo-dyes). These compounds bear oligo(ethylene glycol) segments and are named: RED-PEGM-7, RED-Me, and RED-DIPEGM [27]. Due to specific chemical functionalization, these compounds are able to exhibit quadratic $\chi^{(2)}$ -non-linear optical effects, such as SHG. Details of the sample preparation are given as well as a full comparative morphological and optical study of the three different hybrid films. The experimental findings can be useful for future modifications of the chemical functionality of both the sol-gel host matrix and the azobenzene-based NLO chromophores in the search of novel NLO-active hybrid materials.

2. Experimental section

2.1. Chemical structure of the implemented NLO-chromophores

As shown in Figure 1, the chemical structure of the implemented LC azo-dyes to fabricate sonogel hybrid films is quite similar, these compounds are: (a) [N-methyl-N-4-[(E)-(4-nitrophenyl)diazenyl]phenyl-N-(3,6,9,12,15,18,21-heptaoxadecacos-1-yl)amine], named here RED-PEGM-7, where $R_1 = \text{CH}_3$ and $R_2 = (\text{CH}_2\text{CH}_2\text{O})_7\text{CH}_3$, (b) [1-N,N-dimethylamine-40-nitroazobenzene] named here RED-Me, where $R_1 = R_2 = \text{CH}_3$, and finally (c) [N-4-[(E)-(4-nitrophenyl)diazenyl]phenyl-N,N-di(3,6,9,12,15,18,21-heptaoxadecacos-1-yl)amine], named here: RED-DIPEGM, where $R_1 = R_2 = (\text{CH}_2\text{CH}_2\text{O})_7\text{CH}_3$. The synthetic route employed to obtain RED-PEGM-7 is similar to that used to synthesize the RED-PEGM- n ($n = 3, 8, 10$) compounds (see [28]). Compounds RED-PEGM-7 and RED-Me show a powder-like structure at room temperature, whereas RED-DIPEGM exhibits a viscous LC-state. The corresponding dipole moments were calculated by semi-empirical methods (AM1 and PM3), giving high dipole moment values ranging from 9 to 11 D as shown in Table 1.

2.2. Preparation of hybrid NLO-films

2.2.1. Synthesis of a catalyst-free sonogel network as a host material for LC azo-dyes

The sol-gel method has been frequently used to synthesize amorphous SiO_2 based on the hydrolysis

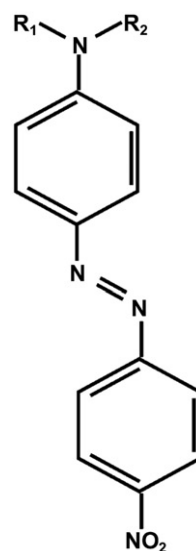


Figure 1. Molecular structure for RED-PEGM-7 ($R_1 = \text{CH}_3$, $R_2 = (\text{CH}_2\text{CH}_2\text{O})_7\text{CH}_3$), RED-ME ($R_1 = R_2 = \text{CH}_3$), and RED-DIPEGM ($R_1 = R_2 = (\text{CH}_2\text{CH}_2\text{O})_7\text{CH}_3$).

of different precursors as tetraethylortosilicate (TEOS) and tetramethoxysilane (TMOS), followed by condensation reaction of the hydrolyzed species. Both hydrolysis and condensation reactions occur normally in the presence of acidic or basic catalysts; for example, ethanol and methanol, which are commonly used as standard solvents for the precursor and water reactants. This methodology has been widely adopted as a suitable way to obtain glassy doped material with acceptable optical and mechanical quality. Fundamental and experimental details for the sol-gel synthesis of SiO_2 can be extensively found in the literature [29,30]. On the other hand, several articles reporting emulsification of the reactive mixtures induced by ultrasonic irradiation have been published in recent years, where no solvents are used [31,32]. In this contribution, a novel approach, recently developed in our research group for the preparation of highly pure SiO_2 sonogels is exploited [24,25]. In this case, the use of both solvents and catalysts is fully suppressed and the hydrolyzed species are substituted by molecular radicals generated by ultrasound irradiation. Thus, these materials have many advantages to fabricate SiO_2 networks with optical quality as host materials for the available LC azo-dyes compounds, as for example: high optical and chemical purity, large porosity, mechanical and thermal stability, etc.

The catalyst-free sonogel route is an easy and low cost methodology; details on the synthesis of this kind of sonogel are given in recent literature [24,25], and basically consists of the following steps: as precursor reactants 25 mL of TEOS (Fluka 99% purity) and 25 mL of distilled water are mixed into a glass vessel and stabilized at 1°C for 1 h before ultrasonic (US) irradiation (these reactants are non-soluble) with a thermal bath used as the cooling system [24,25]. A metallic ultrasound tip (Cole-Parmer-CPX, with 1.25 cm in diameter), carefully located at the TEOS/ H_2O surface interface, provides an effective irradiation power density on the order of 3.2 W cm^{-3} working at 20 kHz. The tip of the ultrasonic-wave generator also acts as an ultrasonic homogenizer. After 3 h of programmed US irradiation (on/off intermittent sequences of 5 s; net irradiation time: 1.5 h), the TEOS/ H_2O temperature mixture¹ is increased up to 6°C due to the energetic US

waves provided to the reactants, afterwards the cooling system was turned off and the sonicated suspension was kept in the reactor vessel at room conditions for ~ 24 h. Thereafter two immiscible phases come out: the upper one, corresponding to unreacted TEOS was removed and eliminated, whereas the more dense lower phase (sol-phase) corresponding to a stable colloidal suspension and containing the sonicated induced hydrolyzed product (OH-TEOS) is capable of producing (after drying and condensation/polymerization) a highly pure SiO_2 amorphous network. In fact, in order to fabricate hybrid glasses, the chromophore doping must be performed in the liquid sol-phase; hence, the dopant solution should be previously prepared. It has been noted that tetrahydrofuran (THF) based organic dopant solutions perform well in order to develop the hybrid structures [25]. These chromophore solutions can be added afterwards and ultrasonically mixed with the OH-TEOS colloidal suspension in order to start the inclusion of dopants within the porosity of the forming SiO_2 matrix.

2.2.2. Fabrication of poled azo-dye based SiO_2 hybrid thin films for NLO applications

Firstly, in order to avoid clusters or inadequate dissolved material, the doped sol mixture was filtered through a $0.22 \mu\text{m}$ Teflon membrane filter before applying a spin-coating procedure on indium-tin-oxide (ITO) glass substrates (substrate dimensions of $2 \times 2.5 \times 0.3 \text{ cm}^3$). The homemade spin-coating system was programmed to deposit one layer of the filtered doped sol at 1000 rpm for 4 s, and each film sample was slowly dried at room temperature for one day.² Under these conditions, average film thicknesses of $\sim 0.3 \mu\text{m}$ can be obtained. Subsequently, since the obtained hybrid films possess an average amorphous structure with poor chromophore alignment due to centrifugal forces, it is necessary to induce strong molecular alignment (perpendicular to the substrate surface) in order to provoke non-centrosymmetric polar order within the hybrid film structure, as required for quadratic NLO effects. A well-established methodology to achieve such molecular ordering is the so-called corona poling technique; this implements an open temperature-controlled oven equipped with a vertical non-oxidable iron needle acting as electrode and the substrate's ITO-layer as anode [33]. Poling conditions implemented to orientate our samples were set as follows: sample temperature was raised from room temperature to $\sim 160^\circ\text{C}$, the applied voltage was 5.00 kV at a needle-sample gap distance of 1 cm; these conditions were kept for 30 min. Thereafter the sample was cooled to room conditions maintaining the same voltage in order to conserve the molecular ordering as

Table 1. Dipole moments of the azo-dyes calculated by semi-empirical (AM1 and PM3) methods.

| Azo-dye | AM1 (D) | PM3 (D) |
|------------|---------|---------|
| RED-PEGM-7 | 10.2 | 8.16 |
| RED-Me | 9.40 | 9.02 |
| RED-DIPEGM | 11.32 | 8.29 |

high as possible. At this point samples were ready for quadratic SHG characterization via the Maker-fringe technique.

2.3. Physical characterization techniques

2.3.1. Morphological AFM analysis

Standard physical characterization techniques were applied to pure sonogel reference samples and hybrid composites in order to determine their structural and physical properties: the morphology of the films was studied by atomic force microscopy (AFM) (Park AutoProbe CP equipment), where the acquisition of images was performed in non-contact mode with an interaction force applied between the sample and the AFM tip of 1.5 nN. The AFM system was equipped with a SiN sharpened Microlever™ tip with typical force constant of 0.05 N and resonant frequency of 22 kHz which specify the mechanical characteristics of the used cantilever (typical constants of the instrument).

2.3.2. Linear and nonlinear optical analysis

Linear optical absorption spectra in reference and hybrid samples were obtained in the 200–1100 nm range using a double beam Shimadzu UV-Vis spectrophotometer, taking air in the reference beam. The second-order optical nonlinearity of the hybrid films were determined by SHG measurements. The SHG experimental device is schematically shown in Figure 2. The set-up is constituted by a commercial Q-switched Nd:YAG laser system (Surelite II from Continuum, $\lambda_\omega = 1064$ nm, repetition rate of 10 Hz and a pulse width of $\tau \sim 22$ ns), which provides the fundamental wave. Typical pulse powers of ~ 100 μ J were filtered in order to irradiate the samples by means of a $f = 5$ mm

focusing lens, thus peak irradiances on the order of 10 MW cm $^{-2}$ were achieved at the focal spot on the hybrid composites. This value was slightly below the energy damage threshold supported by the samples under strong focused beam irradiation. The polarization of the fundamental beam (parallel P or perpendicular S polarizing geometry) was selected by means of an IR-coated Glan-laser polarizer and a $\lambda/2$ half-wave retarder. A second polarizer was used as analyzer allowing the characterization of the SHG signals (P polarization). The second harmonic waves (at $\lambda_{2\omega} = 532$ nm) were detected by a sensitive photomultiplier tube (PMT, Hamamatsu R-928) behind interferential optical filters (centered at 532 ± 5 nm). The SHG device was calibrated by means of a Y -cut alpha-quartz crystal, wedged in the d_{11} -direction ($d_{11} = 0.64$ pm V $^{-1}$), which is commonly used as an NLO reference standard via the Maker-fringe method [36]. The second harmonic intensity of the poled film relative to the quartz crystal, neglecting multiple bounding reflections, is given by [36]:

$$\frac{I_s^{2\omega}}{I_q^{2\omega}} = \pi^2 \chi_{\text{eff}}^{(2)} L_s^2 \exp(-\alpha_s^{2\omega} L_s) \times \frac{|\text{sinhc}[(\alpha_s^{2\omega} + i\Delta B_s)L_s/2]^2 | T_s \epsilon_q^\omega (\epsilon_q^{2\omega})^{1/2}}{4 \chi_q^2 L_{\text{qc}}^2 \sin^2(\pi L_s/L_{\text{qc}}) T_q \epsilon_s^\omega (\epsilon_s^{2\omega})^{1/2} \cos^2 \theta_s}, \quad (1)$$

where $\chi_{\text{eff}}^{(2)}$ is the effective second-order susceptibility, L_s is the sample thickness, α is the attenuation constant, ΔB is the phase mismatch between the fundamental (ω) and second harmonic (2ω) waves, $\text{sinhc}(x) = [\sinh(x)]/x$, T is the product of the electromagnetic power transmission factors of the fundamental and second harmonic waves, ϵ is the permittivity, L_{qc} is the coherence length of the quartz reference (~ 22 μ m) and θ_s is the angle between the boundary normal and the direction of phase propagation inside

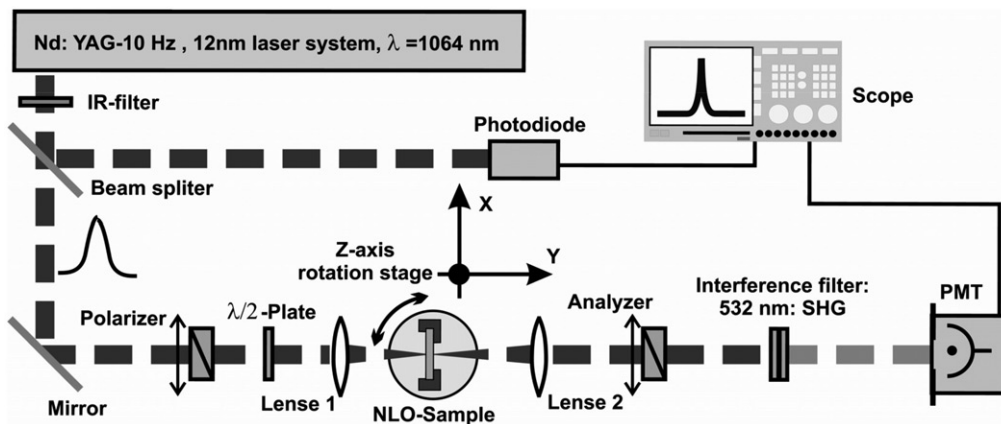


Figure 2. Experimental set-up for SHG measurements in hybrid thin films.

the film. The subscripts s and q refer to the sample and quartz, respectively. If the poled film thickness is thinner than its characteristic coherence length, the value of the χ_{eff}/χ_q ratio is given by [36]:

$$\frac{\chi_{\text{eff}s}^{(2)}}{\chi_q^{(2)}} = \frac{d_{33,s}}{d_{11,q}} = \left(\frac{I_s}{I_q}\right)^{1/2} \frac{L_{\text{qc}}}{L_s} \times \frac{2T_q^{1/2} n_s^{3/2} \cos \theta_s}{\pi \sinh(\alpha_s^{2\omega} L_s/2) \exp(-\alpha_s^{2\omega} L_s/2) n_q^{3/2}}, \quad (2)$$

if absorption effects are neglected, this becomes:

$$\frac{\chi_{\text{eff}s}^{(2)}}{\chi_q^{(2)}} = \frac{d_{33,s}}{d_{11,q}} \approx \left(\frac{I_s}{I_q}\right)^{1/2} \frac{L_{\text{qc}}}{L_s} F, \quad (3)$$

here the $d_{11,q}$ is the well known coefficient of the quartz reference (0.64 pm V^{-1}) and F is the correction factor for the apparatus and is equal to 1.3 when $L_{\text{qc}} \gg L_s$. Thus, a simple relation can be used to estimate the quadratic susceptibility of a new substance relative to a reference standard material.

3. Results and discussion

3.1. Morphological AFM analysis

The poled coated films present homogeneity and good adherence to the substrate. The AFM inspection of the developed film surfaces are shown in Figures 3(a)–(d): Figure 3(a) shows the pure sonogel reference film ($0.42 \mu\text{m}$ in thickness), where a flat and homogeneous surface with only a few defects can be observed. Figures 3(b)–(d) shows the developed hybrid film for RED-PEGM-7 ($0.27 \mu\text{m}$ average thickness), RED-ME ($0.33 \mu\text{m}$ average thickness), and RED-DIPEGM ($0.30 \mu\text{m}$ average thickness), respectively. It is clear that all hybrid films exhibit smaller thicknesses than the respective coherence lengths observed in similar dyes (in the order of $\sim 10 \mu\text{m}$) [37]. Hybrid films show in general a very different surface structure compared to the reference (undoped) film; in fact, the hybrid surface textures present a more irregular structure with increased roughness and smaller film thicknesses. This is due to the higher viscosity of the undoped sonogel. Nevertheless, the hybrid films still exhibit a homogeneous structure with regular deposition, showing only some defects (more pronounced in the case of the RED-DIPEGM based film) and regular grain size distribution, which make them appropriate to perform optical characterizations. Table 2 summarizes some structural parameters measured by AFM of the studied film samples.

3.2. UV-Vis spectral characterization

The UV-Vis absorption spectra of the films before and after performing electrical poling are shown in Figure 4. In general, electrical poling provokes a decrease in the absorption intensity and a small shift of the absorption maximum (λ_{MAX}) to longer wavelengths [33]. In fact, as shown in Figures 4(a)–(c), the comparative absorption spectra exhibit a clear intensity decrease obtained after electrical poling of the samples (hypochromic shift at λ_{MAX}), a slight shift toward longer wavelengths (bathochromic shift) can be observed in Figure 4(b). The electrostatic field aligns the chromophore dipoles in the direction of the poling field, leading to a change (decrease) in the intensity of the absorption spectrum, i.e. to dichroism [38,39]. In general, this orientation is maintained, depending on the T_g values of the chromophores. In this case, the monomeric azo-dyes embedded within the host matrix exhibit a stable orientation as the temperature is lowered. The permanent part of the hypochromic shift observed after poling is mainly attributed to the permanent alignment of the chromophores in the polymer host.

In order to test if there are any other causes influencing the absorptive properties of the films, such as temperature chromophore decomposition, temperature phase or oxidation transitions, etc., the films were annealed to the same temperature and time without applying DC fields. No sign of absorption reduction and spectral shifts were observed. Therefore, the absorption intensity changes can be only attributed to the azo-benzene molecular orientation within the film structure due to electrical poling. Thereafter, the dipole moments of the chromophores are aligned which led to a change of the order parameter ϕ defined by: $\phi = 1 - A_{\perp}/A_0$, where A_0 and A_{\perp} are the maximum film absorbances before and after electrical poling, respectively. This parameter is useful to estimate the degree of chromophore orientation; according to this formula the order parameters of our poled samples were evaluated as: 0.141, 0.110, and 0.126 for the RED-PEGM-7, RED-ME, and RED-DIPEGM based hybrid films, respectively. These parameters are rather low compared to other LC-compounds; they are however high enough to produce an effective average orientation within the hybrid structure and to observe any induced ferroelectric polar order suitable for NLO-SHG measurements.

3.3. SHG-nonlinear optical measurements

Finally, a SHG test was performed on the poled hybrid film systems in order to investigate the quadratic NLO performance of our developed films, and most importantly, to verify any possible permanent

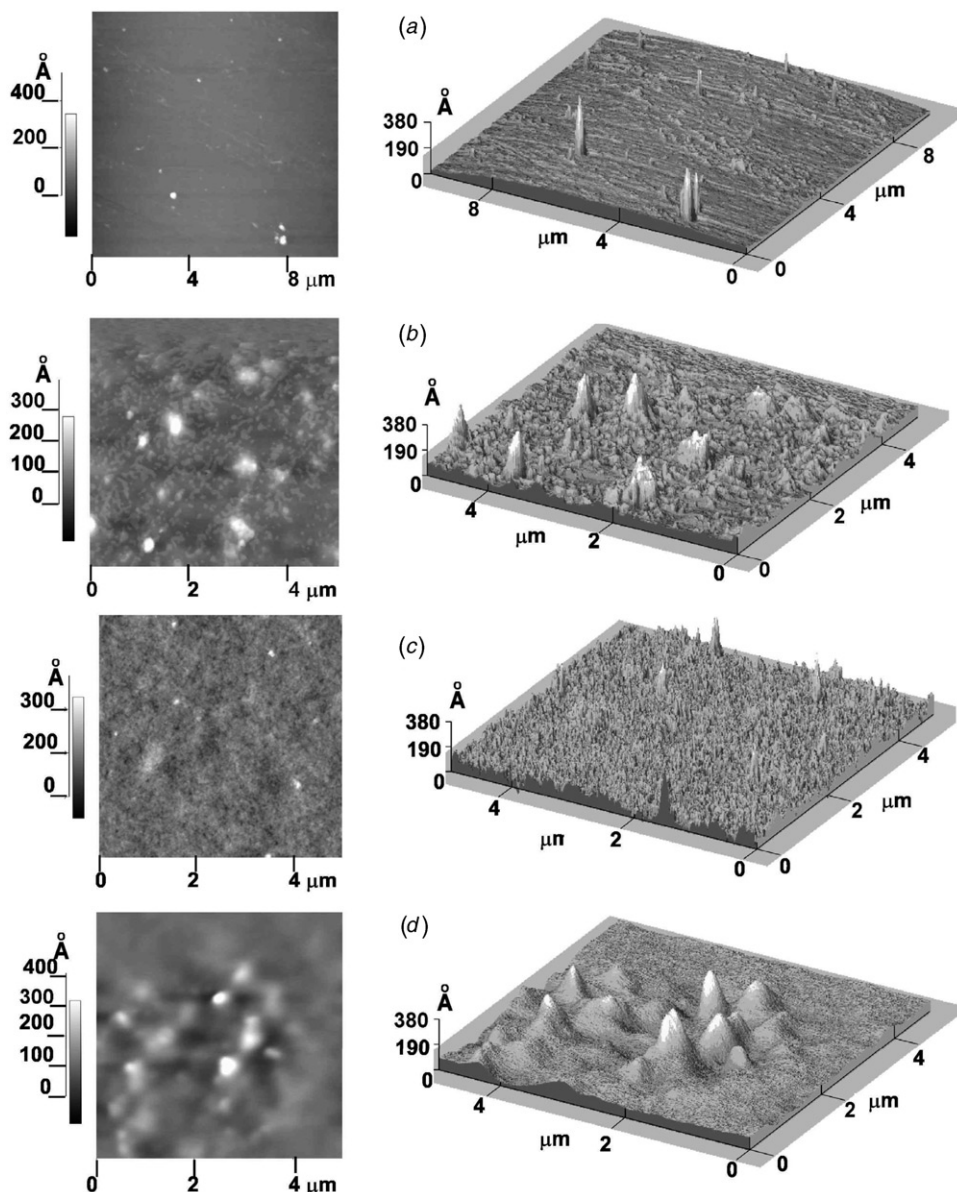


Figure 3. AFM micrographs of the developed hybrid film samples (2D and 3D views): (a) pure sonogel reference film sample, (b) RED-PEGM-7 based hybrid film, (c) RED-ME based hybrid film, and (d) RED-DIPEGM based hybrid film.

Table 2. Average thickness and roughness in fabricated pure reference and hybrid thin films.

| Azo-dye | Film thickness (μm) | Film roughness (\AA) |
|------------------------|----------------------------------|---------------------------------|
| Pure reference sonogel | 0.42 | 60 |
| RED-PEGM-7 | 0.27 | 150 |
| RED-Me | 0.33 | 90 |
| RED-DIPEGM | 0.30 | 140 |

molecular ordering achieved by the implemented monomeric compounds within the sonogel network through the electrical poling procedure. This is interesting since the monomeric chemical structure of the

compounds exhibits a LC-azo-dye behavior and would be very promising in order to achieve stable and low cost materials for NLO application via the sonogel route. In fact, stable measurable SHG signals were detected for two of the hybrid samples, indicating a stimulated and permanent ordering of the guest molecules induced by the corona poling process as shown in Figure 5 ($P/\text{In}-P/\text{Out}$ polarizing geometry). In this figure one can appreciate the SHG activity of the samples as a function of the incidence angle according to the Maker-fringe method (Figure 5(a)). On the other hand, Figure 5(b) shows the estimated NLO $\chi_{\text{eff}}^{(2)}$ macroscopic susceptibility coefficients evaluated from the Maker-fringes for the sonogel hybrid

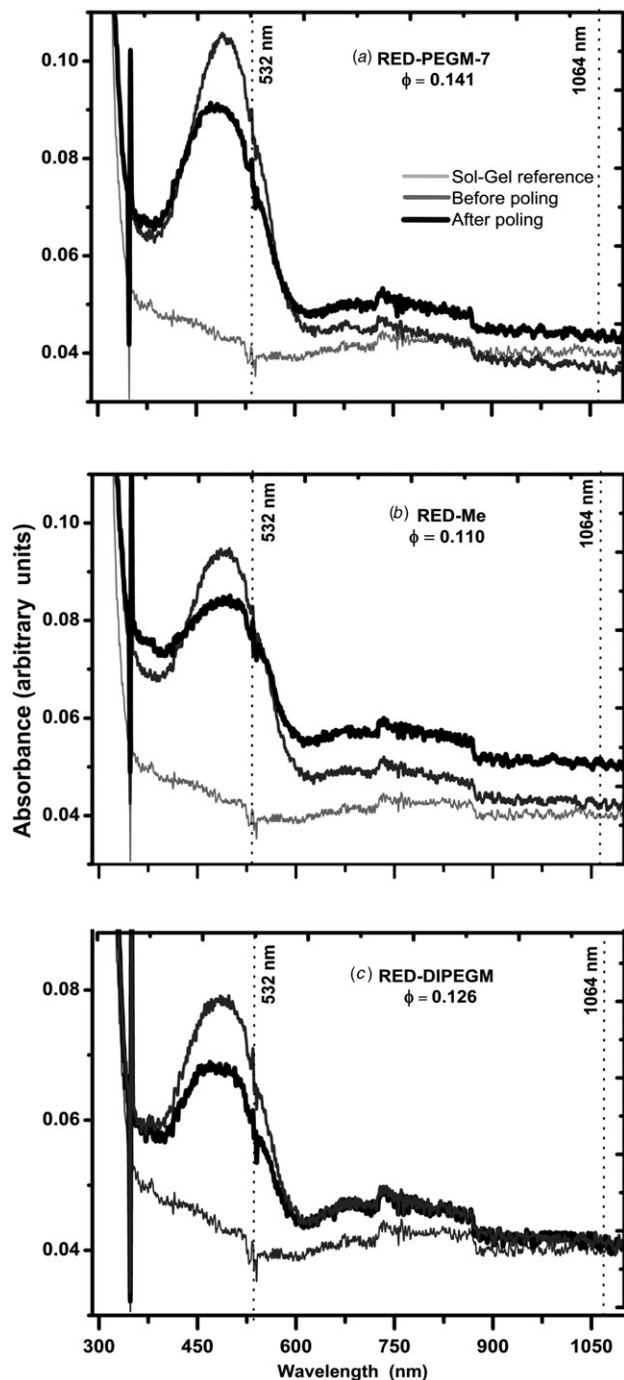


Figure 4. Comparative UV-Vis absorption spectra of the pure sonogel reference and the hybrid film samples, before and after performing electrical poling: (a) RED-PEGM-7 based hybrid film, (b) RED-ME based hybrid film, and (c) RED-DIPEGM based hybrid film.

samples (an estimated experimental error of about 15% is considered), significant SHG measurements were performed implementing *P*-In/*P*-Out fundamental/SHG³ beam polarization geometries due to the optimal optical polarization matching with the long

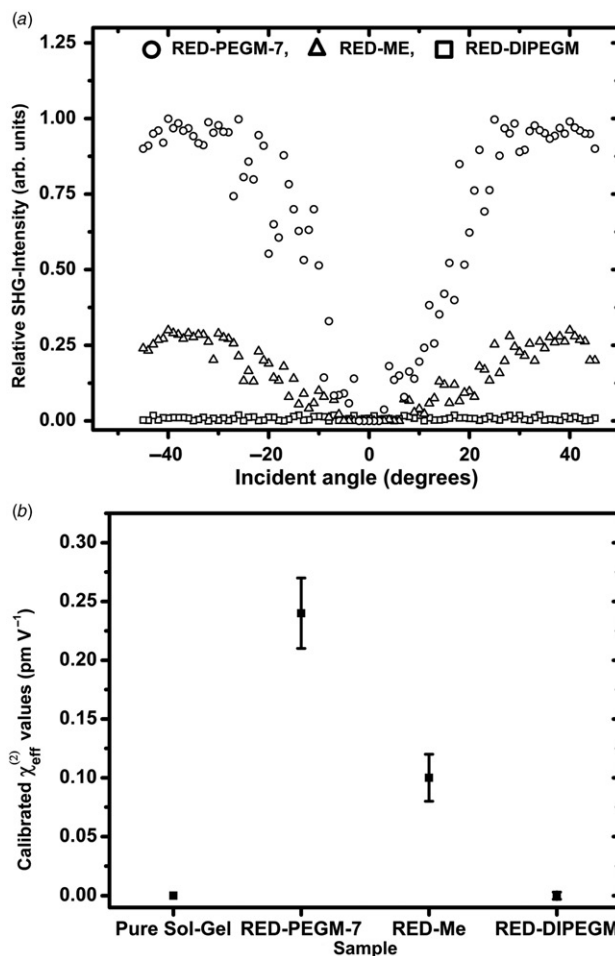


Figure 5. SHG/NLO-measurements performed on the hybrid thin films according to the Maker-fringe technique: (a) angle dependent SHG measurements (*P*-In/*P*-Out polarizing geometry) and (b) calibrated $\chi_{\text{eff}}^{(2)}$ NLO coefficients.

molecular axis of the compounds. As expected, no SHG signals were observed for the pure sonogel reference sample due to its inherent amorphous centro-symmetric structure. This amorphous glassy structure has been verified in others works by X-ray diffraction (XRD) (not shown here, see [24]). By contrast, important SHG signals can be obtained from the developed hybrid structures, where relatively high $\chi_{\text{eff}}^{(2)}$ coefficients were evaluated for the *P*-In/*P*-Out polarization geometry (considerably stronger than those obtained by surface SHG effects, which are only observable by lock-in amplified measurements). It is observed that the SHG signals do not exhibit a clear oscillating behavior (usual from non-phase matched Maker-fringe experiments); this is partially due to the absorptive properties of the media at the SHG wavelength and strong scattering effects. For these reasons only the average effective $\chi_{\text{eff}}^{(2)}$ parameters were evaluated according to Equation (3) relative to the reference sample.

4. Conclusions

An adequate insertion of the implemented LC azo-dyes within the sonogel matrix to produce optically active hybrid films has been achieved as monitored by AFM, absorption spectroscopy and the NLO-SHG Maker-fringe technique. The poled coated hybrid films present homogeneity and good adherence to the ITO coated glass substrates, showing a very different surface morphology compared to the reference (undoped) film, where the hybrid surface textures present a more irregular structure with increased roughness and smaller film thicknesses. The corona-poling method was effective to induce stable molecular ordering in the RED-PEGM-7 and RED-Me based hybrid structures, appropriate for the emergence of quadratic NLO-SHG effects. Although the RED-DIPEGM compound shows the higher dipole moment among the studied dyes, due to strong molecular aggregation and high viscosity, no SHG was observed for the respective hybrid, whereas non negligible quadratic nonlinearities were measured for the RED-Me and RED-PEGM-7 based hybrid films. The lower absorption observed for the RED-PEGM-7 based hybrid has enabled it to exhibit highest quadratic NLO coefficient ($\chi_{\text{eff}}^{(2)} \approx 0.24 \text{ pm V}^{-1}$). The implemented molecular azo-dye compounds have been studied recently in anodic alumina membrane (AAM) based hybrid systems [27], showing similar performance for the NLO characterization under this molecular confinement. Phenomenologically, it has been very interesting to achieve stable monomeric molecular ordering with the sonogel network; nevertheless, additional structural investigations should be performed in order to further understand the interaction of this LC azo-dye family and other guest molecular systems (monomers and polymers) within the sonogel environment. Finally, we can observe that the sonogel host system has provided thermal and mechanical molecular stability protecting the active chromophores from the environment and preserving their optical properties, thus producing sol-gel hybrid glasses suitable for optical applications.

Acknowledgements

The authors are grateful to Dr Neil Bruce for English revision of the manuscript. This work was supported by projects SEP-CONACyT (Grant 82808-F) and PAPIIT-DGAPA-UNAM (Grant IN-IN115508). O.G. Morales-Saavedra acknowledges financial support from the DAAD academic organization (Germany).

Notes

1. The TEOS/H₂O mixture obtained after sonication is a homogeneous opaque suspension containing both the

sonochemically reacted and unreacted molecular species from the constituting reactants. Note that despite the fact that the cooling system is always on during sonication, the intermittent US-irradiation sequences of 5 s allow the system to cool down in order to avoid excessive reaction temperatures promoted by intense US irradiation. These intermittent irradiation sequences also provide adequate silence periods for recombination of the formed molecular species, giving rise to an increase of hydrolyzed Si-based molecular compounds, which form after condensation/polymerization the SiO₂ glassy network [24].

2. The slow drying process of the samples performed at room temperature has proven to be efficient in order to produce quality film structures with adequate morphology suitable for optical characterization as verified by AFM microscopy (see Section 3.1). On the other hand, it has also been proven that negligible water residuals remain within the porous sonogel glassy structure [24], which in any case are fully eliminated as the film samples are heated up to 160°C for corona-poling processing or are non-active for quadratic NLO-SHG effects.
3. Note that for the *S*-In/*P*-Out fundamental/SHG polarizing geometry SHG data are not reported. In fact, the strong absorption and light scattering produced by the hybrid samples affected the accuracy of the weaker SHG signals observed under these experimental conditions.

References

- [1] Marder, S.R.; Kippelen, B.; Jen, A.K.Y.; Peyghambarian, N. *Nature* **1997**, *388*, 845–851.
- [2] Kusk, M. All-optical Materials and Devices. In *Organic Thin Films for Waveguiding Nonlinear Optics*; Kajzar, F., Swalen, J.D., Eds.; CRC Press: The Netherlands, 1996; pp 759–820.
- [3] Dini, D.; Hanack, M. Physical Properties of Phthalocyanine-based Materials. In *The Porphyrin Handbook*; Kadish, K.M., Smith, K.M., Guillard, R., Eds.; Academic Press: USA, 2003; Vol. 17, pp 22–31.
- [4] Chang, C.-C.; Chen, C.-P.; Chou, C.-C.; Kuo, W.-J.; Jeng, R.-J. *Polym. Rev.* **2005**, *45*, 125–170.
- [5] Caruso, U.; Casalboni, M.; Fort, A.; Fusco, M.; Panunzi, B.; Quatela, A.; Roviello, A.; Sarcinelli, F. *Opt. Mater.* **2005**, *27*, 1800–1810.
- [6] Lindsay, G.A.; Singer, K.D., Ed. *Polymers for Second Nonlinear Optics*; ACS Symposium Series No. 601, American Chemical Society: Washington, DC, 1995; p 20.
- [7] Miller, R.D. Poled Polymers for X(2) Applications. In *Organic Thin Films for Waveguiding Nonlinear Optics*; Kajzar, F., Swalen, J.D., Eds.; Gordon and Breach Publishers: San Jose, USA, 1996; pp 329–456, Chapter 8.
- [8] Marder, S.R.; Sohn, J.E.; Stucky, G.D. *Materials for Nonlinear Optics, Chemical Perspectives*; ACS Symposium Series No. 455, American Chemical Society: Washington, DC, 1991.
- [9] Rabek, J.K. *Photochemistry and Photophysics*; CRC Press: Boca Raton, FL, 1990; Vol. 2, p 119.
- [10] Yesodha, S.K.; Pillai, C.K.S.; Tsutsumi, N. *Prog. Polym. Sci.* **2004**, *29*, 45–74.

- [11] Natansohn, A.; Rochon, P. *Chem. Rev.* **2002**, *102*, 4139–4176.
- [12] Huang, S.D.; Xiong, R.G. *Polyhedron* **1997**, *16*, 3929–3939.
- [13] Chen, Y.C.; Juang, T.Y.; Dai, S.A.; Wu, T.-M.; Lin, J.J.; Jeng, R.-J. *Macromol. Rapid. Commun.* **2008**, *29*, 587–592.
- [14] Kajzar, F.; Lee, K.S.; Jen, A.K.Y. *Adv. Polym. Sci.* **2003**, *161*, 1–85.
- [15] Fukuda, T.; Matsuda, H.; Kimura, T.; Shiraga, T.; Kato, M.; Nakanishi, H. *Polym. Advan. Technol.* **2000**, *11*, 583–588.
- [16] Rivera, E.; Carreón-Castro, M.P.; Rodríguez, L.; Cedillo, G.; Fomine, S.; Morales-Saavedra, O.G. *Dyes Pigments* **2007**, *74*, 396–403.
- [17] Schwartz, H.; Mazor, R.; Khodorkovsky, V.; Shapiro, L.; Klug, J.T.; Kovalev, E.; Meshulam, G.; Berkovic, G.; Kotler, Z.; Efrima, S. *J. Phys. Chem. B* **2001**, *105*, 5914–5921.
- [18] Xie, J.; Deng, X.; Cao, Z.; Shen, Q.; Zhang, W.; Shi, W. *Polymer* **2007**, *48*, 5988–5993.
- [19] Carella, A.; Centore, R.; Mager, L.; Barsella, A.; Fort, A. *Organ. Electron.* **2007**, *8*, 57–62.
- [20] Canva, M.; Georges, P.; Le Saux, G.; Brun, A.; Larrue, D.; Zarzycki, J. *J. Mat. Sci. Lett.* **1991**, *10*, 615–618.
- [21] Shea, K.J.; Loy, D.A. *Chem. Mater.* **2001**, *13*, 3306–3319.
- [22] Choi, D.H.; Park, J.H.; Lee, J.H.; Lee, S.D. *Thin Solid Films* **2000**, *360*, 213–221.
- [23] Cui, Y.; Li, B.; Yu, C.; Yu, J.; Gao, J.; Yan, M.; Chen, G.; Wang, Z.; Qian, G. *Thin Solid Films* **2009**, *517*, 5075–5078.
- [24] Ocotlán-Flores, J.; Saniger, J.M. *J. Sol-Gel Sci. Tech.* **2006**, *39*, 235–240.
- [25] Morales-Saavedra, O.G.; Rivera, E.; Flores-Flores, J.O.; Castañeda, R.; Bañuelos, J.G.; Saniger, J.M. *J. Sol-Gel Sci. Tech.* **2007**, *41*, 277–289.
- [26] Zhang, H.X.; Lu, D.; Fallahi, M. *Appl. Phys. Lett.* **2004**, *84*, 1064–1066.
- [27] Morales-Saavedra, O.G.; Mata-Zamora, M.E.; Rivera, E.; García, T.; Bañuelos, J.G.; Saniger-Blesa, J.M. *Dyes Pigments* **2008**, *78*, 48–59.
- [28] Natansohn, A.; Rivera, E.; Belletête, M.; Durocher, G. *Can. J. Chem.* **2003**, *81*, 1076–1082.
- [29] Saenz, A.; Salas, P.; Rivera, E.; Montero, M.L.; Castaño, V.M. *Mater Technol.* **2003**, *18*, 25–29.
- [30] Pomogailo, A.D. *Colloid J.* **2005**, *67*, 658–677.
- [31] Blanco, E.; Esquivias, L.; Litrán, R.; Piñero, M.; Ramírez-del-Solar, M.; De La Rosa-Fox, N. *Appl. Organometal. Chem.* **1999**, *13*, 399–418.
- [32] De La Rosa-Fox, N.; Morales-Florez, V.; Pinero, M.; Esquivias, L. *Nanostructured Sonogels Key Eng. Mater.* **2009**, *391*, 45–78.
- [33] Giacometti, J.A.; Fedosov, S.N.; Costa, M.M. *Braz. J. Phy.* **1999**, *29*, 269–280.
- [34] Kajzar, F.; Lee, K.S.; Jen, A.K.Y. *Adv. Polym. Sci.* **2003**, *161*, 1–85.
- [35] Shen, Y.R. *The Principles of Nonlinear Optics*; Wiley: New York, 1984.
- [36] Mortazavi, M.A.; Knoesen, A.; Kowel, S.T.; Higgins, B.G.; Dienes, A. *J. Opt. Soc. Am. B* **1989**, *6*, 733–741.
- [37] Ju, J.J.; Kim, J.; Do, J.Y.; Kim, M.-S.; Park, S.K.; Park, S.; Lee, M.-H. *Opt. Lett.* **2004**, *29*, 89–91.
- [38] Pérez-Martínez, A.L.; Ogawa, T.; Aoyama, T.; Wada, T. *Opt. Mater.* **2009**, *31*, 912–918.
- [39] Yamaoka, K.; Charney, E. *J. Am. Chem. Soc.* **1972**, *94*, 8963–8974.